

# A simple method of determination of the degree of gas mixing by numerical Laplace inversion and Maple®

M. WÓJCIK\* and M. SZUKIEWICZ

The Faculty of Chemistry, Department of Chemical and Process Engineering, Rzeszow University of Technology,  
al. Powstancow Warszawy 6, 35-959 Rzeszow, Poland

**Abstract.** This article presents a new efficient method of determining values of gas flow parameters (e.g. axial dispersion coefficient,  $D_L$  and Péclet number,  $Pe$ ). A simple and very fast technique based on the pulse tracer response is proposed. It is a method which combines the benefits of a transfer function, numerical inversion of the Laplace transform and optimization allows estimation of missing coefficients. The study focuses on the simplicity and flexibility of the method. Calculations were performed with the use of the CAS-type program (Maple®). The correctness of the results obtained is confirmed by good agreement between the theory and experimental data for different pressures and temperature. The CAS-type program is very helpful both for mathematical manipulations as a symbolic computing environment (mathematical formulas of Laplace-domain model are rather sophisticated) and for numerical calculations. The method of investigations of gas flow motion is original. The method is competitive with earlier methods.

**Key words:** inverse boundary value problem, the Gaver-Stehfest algorithm, axial gas dispersion coefficient, Péclet number, CAS program.

## 1. Introduction

The Laplace transform is an important integral transform in engineering applications in mechanics, physics, chemistry, biology etc. It is a very powerful tool of mathematics for solving differential and integral equations. Nevertheless, application of this technique in practice is limited, because an analytical inversion of problems to the time domain can be difficult or even impossible to obtain and then only numerical methods can be applied. Indeed, there are numerous inverse Laplace transform numerical algorithms that can be used to find a time-domain solution for a specific type of problems in many areas of engineering mathematics and engineering systems e.g. for gas and liquid flow, for mass and energy transport. For example, the Gaver-Stehfest method is a popular numerical inversion algorithm used in groundwater flow and petroleum engineering applications [1]. The method was applied successfully to solve various problems in chemistry (modelling of electrochemical systems, e.g. [2]), economy (option pricing formulas, e.g. [3]), geophysics (electromagnetic calculations, e.g. [4]), electrical engineering (telecommunication problems, e.g. [5]). In the study [6], the Stehfest and Dubner and Abate algorithms were applied to solving a suitable model of tracer transport in heterogeneous media, oil and geothermal reservoirs, in groundwater aquifers. The Stehfest, the Honig and Hirdes, and Zakian's methods were recommended for the dispersion-dominated problems, but for radial dispersion problems – the de Hoog,

the Talbot, and the Simon methods [7]. Chiang [8] tried out many methods (the Schapery, the Widder, the Koizumi, the Weeks, and the Talbot methods) to obtain solution of groundwater problems. Escobar et al. [9] presented the comparison of two algorithms, the Stehfest's and Iseger's method to solve two oil-industry reservoir models in the Laplace domain. Chen et al. [10] employed the Crump algorithm to obtain the solution of the radial dispersion in the real-time domain from the Laplace domain. The de Hoog algorithm was used to determine the fate and transport of groundwater contaminants (i.e. chromium), biotracers and microorganisms [11]. Taiwo et al. [12] compared two methods, the Honig and Hirdes, and Zakian's method to four typical chemical engineering problems. Also, Zakian's algorithm was used to determine of the kinetic parameters for the adsorption of human serum albumin [13]. The use of the Hosono method in determining the signal velocity in dispersive pulse propagation was presented in study [14]. Summarizing, the mentioned algorithms are suitable for a wide spectrum of applications.

In this study a new simple method for the determination of parameters characterizing gas flow motion is presented (axial dispersion coefficient or a Péclet number). The approach is based on authors' transient mathematical model of gas flow motion within Micromeritics' AutoChem 2950HP instrument. Differential equations describing gas flow are transformed into Laplace domain to transfer function form. The Gaver-Stehfest algorithm is chosen (numerical tests that confirmed its efficiency for gas flow problems have been presented by Wójcik et al. [15]). The model solutions are optimized to fit to experimental results. The method proposed is simple and convenient for evaluating model coefficients. It is competitive with other methods.

\*e-mail: wojcik.mm@op.pl

Manuscript submitted 2018-03-11, revised 2018-09-28, initially accepted for publication 2018-10-22, published in April 2019.

## 2. Mathematical model

The simplified scheme of measuring system for experiments is shown in Fig. 1.

- Mathematical model takes into account internal construction of an instrument. The system consists of the following elements:
- 1) an U-shaped element called *vessel*. The vessel is fixed directly to the valve (2), and it consists of two steel pipes (1a) and (1b). The part of larger diameter (1a) is usually filled with porous pellets but in the present experiment it is empty.
  - 2) the 8-way valve
  - 3) the sample loop
  - 4) pipes
  - 5) the thermal conductivity detector (TCD).

### 2.1. Nomenclature

- $c(L_1 + L_2 + L_3, t)$  outlet concentration of the tracer in the gas phase, (mol/m<sup>3</sup>)
- $\bar{c}(L_i, s)$  concentration in Laplace domain,  $i = 1 \dots, 3$
- $c_0$  inlet concentration of the tracer, (mol/m<sup>3</sup>)
- $c_T$  concentration of the tracer, (mol/m<sup>3</sup>),  $c_T = P/(R_g \cdot T)$
- $D_{L,i}$  axial dispersion coefficient in  $i$ -th zone, (m<sup>2</sup>/s),  $i = 1 \dots, 3$
- $d_{w,i}$  diameter of the zone, (m),  $i = 1 \dots, 3$
- $F_v$  volumetric flow rate, (m<sup>3</sup>/s)
- $G_i(s)$  transfer function for zone,  $i = 1 \dots, 3$
- $L_i$  length of  $i$ -th zone, (m),  $i = 1 \dots, 3$
- $P$  pressure, (Pa)
- $R_g$  universal gas constant, (J/(mol K))
- $s$  Laplace transform parameter
- $t$  time, (s)
- $t_p$  time of duration of rectangular pulse, (s)
- $T$  temperature, (K)
- $V_{imp}$  volume of sample loop, (m<sup>3</sup>)
- $v_i$  gas flow velocity, (m/s),  $i = 1 \dots, 3$ ,  $v_i = 4F_v/(\pi \cdot d_{w,i}^2)$ .

In order to create a mathematical model of the gas flow, the unit between the valve (2) and the TCD detector (5) was divided into three separate zones. They differ one to another by geometry, by function, or both. Geometry of the apparatus has been determined on the basis of its technical data and formerly made investigations. A complete list of technical data is presented in Table 1.

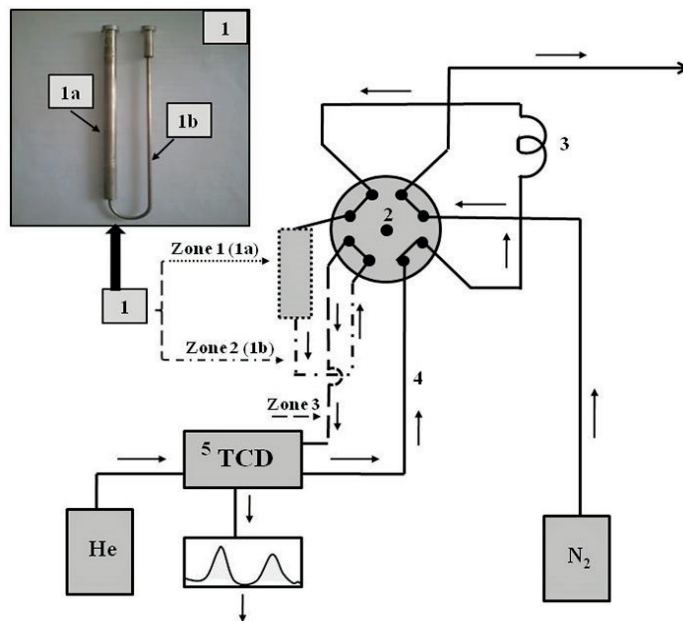


Fig. 1. The simplified schematic representation of apparatus (Mikromeritics' AutoChem 2950HP)

Table 1  
 Technical data

| Number of the zone | Description of the zone                      | $L_i, m$             | $d_{w,i}, m$         |
|--------------------|--|----------------------|----------------------|
| 1                  | vessel, 1a                                   | $1.77 \cdot 10^{-1}$ | $7.65 \cdot 10^{-3}$ |
| 2                  | vessel, 1b                                   | $2.35 \cdot 10^{-1}$ | $1.59 \cdot 10^{-3}$ |
| 3                  | pipe connecting 8-way valve and TCD detector | $5.70 \cdot 10^{-1}$ | $1.59 \cdot 10^{-3}$ |

**2.2. Assumptions of the model.** The model is based on the following assumptions:

- the system is operated under isothermal and isobaric conditions
- gases satisfy the equation of state of an ideal gas
- $D_{L,2}$  is equal to  $D_{L,3}$  due to the same diameters of the pipes.

**2.3. Mass balance of the process.** The mass balance of the tracer (nitrogen) in each zone can be described by the following partial differential equations with appropriate initial and boundary conditions (Table 2).

Table 2  
 Mathematical model

| Equation                      | $\frac{\partial c(x, t)}{\partial t} = D_{L,i} \frac{\partial^2 c(x, t)}{\partial x^2} - v_i \cdot \frac{\partial c(x, t)}{\partial x}$ | 1   | 2   | 3   |
|-------------------------------|---|---|---|---|
| <b><math>i</math>-th zone</b> |   | 1   | 2   | 3   |
| <b>IC</b>                     | $c(x, 0) = 0$   | $c(x, 0) = 0$   | $c(x, 0) = 0$   | $c(x, 0) = 0$   |
| <b>BC1</b>                    | $v_i \cdot c_0 = v_i \cdot c(0^+, t) - D_{L,i} \frac{\partial c(x, t)}{\partial x} \Big _{x=0^+}$                                       | $c(L_1^+, t) = c(L_1^-, t)$                               | $c(L_1^+, t) = c(L_1^-, t)$                                   | $c(L_1 + L_2^+, t) = c(L_1 + L_2^-, t)$                         |
| <b>BC2</b>                    | $\frac{\partial c(x, t)}{\partial x} \Big _{x=L_1^+} = \frac{\partial c(x, t)}{\partial x} \Big _{x=L_1^-}$                             | $\frac{\partial c(x, t)}{\partial x} \Big _{x=L_1^+} = 0$ | $\frac{\partial c(x, t)}{\partial x} \Big _{x=L_1+L_2^-} = 0$ | $\frac{\partial c(x, t)}{\partial x} \Big _{x=L_1+L_2+L_3} = 0$ |

Input concentration  $c_0$  (rectangular signal pulse) is described by:

$$c_0 = \begin{cases} 0 & \text{for } t < 0 \\ c_T & \text{for } 0 \leq t \leq \frac{V_{imp}}{F_v} \\ 0 & \text{for } t > \frac{V_{imp}}{F_v} \end{cases} \quad (1)$$

TCD signal recorded corresponds to.

### 3. Description of the experiments

The aim of an experiment was to determine the effect of mixing during the flow gas inside AutoChem 2950HP instrument. This can help the researcher in interpretation of results of others experiments, where the AutoChem 2950HP has been or will be used. We introduce the rectangular pulse of nitrogen and next investigate its transport and spreading through a tube system. The shape of outlet signal allows for evaluation of axial dispersion coefficient. The more deformation of an outlet signal the larger influence of axial dispersion and the larger value of the coefficient. All the model parameters apart from axial dispersion coefficient  $D_L$  are set in the apparatus (e.g. P, T,  $F_v$ ) or are

presented in the manual of apparatus (e.g.  $V_{imp}$ ,  $d_{w1}$ ,  $d_{w2}$ ,  $d_{w3}$ ); values of others can be easily calculated using them.

The system was flushed for 15–30 minutes with a constant flow of helium (carrier) until a stable TCD signal was received. At the same time, the volume of sample loop ( $2.50 \cdot 10^{-7}$ ;  $5.00 \cdot 10^{-7} \text{ m}^3$ ) was flushed also with a constant flow of nitrogen (tracer). Next, the 8-way valve was opened to allow the flow of helium with the constant volumetric flow rate ( $3.33 \cdot 10^{-7} \text{ m}^3/\text{s}$  at STP) through the sample loop, the zones and the detector TCD. After all, the TCD signal was recorded.

The experiments were conducted in New Chemical Synthesis Institute in Pulawy (Poland) at each combination of process variable:

- pressure:  $1.20 \cdot 10^5$ ;  $2.00 \cdot 10^5$ ;  $3.00 \cdot 10^5 \text{ Pa}$
- temperature: 313; 333; 353 K.

### 4. Results and discussion

Differential equations presented in Table 2 were transformed by Laplace transformation into ordinary differential equations and next analytically solved with appropriate initial and boundary conditions to obtain  $\bar{c}(L_1 + L_2 + L_3, s)$ .

The solution of the model in Laplace domain can be presented as:

$$\frac{\bar{c}(L_1 + L_2 + L_3, s)}{c_0(s)} = G_{1,2}(s) \cdot G_3(s) \quad (2)$$

where

$$G_{1,2}(s) = \frac{\bar{c}(L_1 + L_2, s)}{c_0} = - \frac{4e^{\frac{D_{L,1} \cdot L_1 \cdot v_2 + D_{L,1} \cdot L_1 \cdot v_1}{D_{L,2} \cdot D_{L,1}}} (4D_{L,1} \cdot s - A \cdot v_1 + v_1^2) v_1 \cdot B}{e^a (-4D_{L,1} \cdot A \cdot s - 2 \cdot A \cdot v_1 \cdot v_2) + e^b (4D_{L,1} \cdot A \cdot s + 2 \cdot A \cdot B \cdot v_1 + 2 \cdot A \cdot v_1 \cdot v_2)} \quad (3)$$

$$G_3(s) = \frac{\bar{c}(L_1 + L_2 + L_3, s)}{\bar{c}(L_1 + L_2, s)} = \frac{2C \cdot e^{\frac{(L_1 + L_2 + L_3) \cdot v_3}{D_{L,3}}}}{C \cdot e^{d+f} + v_3 \cdot e^{d-f}} \quad (4)$$

where

$$A = \sqrt{4D_{L,1} \cdot s + v_1^2} \quad (5)$$

$$B = \sqrt{4D_{L,2} \cdot s + v_2^2} \quad (6)$$

$$C = \sqrt{4D_{L,3} \cdot s + v_3^2} \quad (7)$$

$$a = \frac{1}{2} \frac{D_{L,1} \cdot L_2 \sqrt{4D_{L,2} \cdot s + v_2^2} - 2L_1 \cdot D_{L,1} \cdot v_2 - D_{L,1} \cdot L_2 \cdot v_2 - D_{L,2} \cdot L_1 \sqrt{4D_{L,1} \cdot s + v_1^2} - D_{L,2} \cdot L_1 \cdot s}{D_{L,1} \cdot D_{L,2}} \quad (8)$$

$$b = \frac{1}{2} \frac{D_{L,1} \cdot L_2 \sqrt{4D_{L,2} \cdot s + v_2^2} + 2L_1 \cdot D_{L,1} \cdot v_2 + D_{L,1} \cdot L_2 \cdot v_2 + D_{L,2} \cdot L_1 \sqrt{4D_{L,1} \cdot s + v_1^2} + D_{L,2} \cdot L_1 \cdot s}{D_{L,1} \cdot D_{L,2}} \quad (9)$$

$$d = \frac{1}{2} \frac{L_3 \sqrt{4D_{L,3} \cdot s + v_3^2} + 2L_1 \cdot v_3 + 2L_2 \cdot v_3 + L_3 \cdot v_3}{D_{L,3}} \quad (10)$$

The complex function  $\bar{c}(L_1 + L_2 + L_3, s)$  is converted into a real domain applying numerical inverse Laplace transform technique. Since, a relationship between nitrogen concentration and TCD signal was found to be linear for process operating conditions, results of experiment and simulation can be easily compared.

On the basis of previous tests the Gaver-Stehfest algorithm is chosen as the suitable numerical method of inverse Laplace transform [16]. The investigations made included accuracy tests for arbitrary chosen functions and for a simplified model of a real gas flow. Based on the results obtained the authors sug-

gest to use  $N = 30$  as an optimal value. The parameter  $N$  is the number of terms used in Gaver-Stehfest algorithm [1–3].  $N$  must be an even integer it is usually chosen by trial and error method. If  $N$  rises, accuracy of results increases at first, but then it gets declining due to round-off errors.

The unknown values of model parameters are determined using the inner optimization procedure *NLPsolve* of the program Maple®. The estimated parameters were  $D_{L,i}$ . Typical results are presented in Fig. 2. A very good fit is observed between numerical and experimental curves. It indicates that the model adequately describes the experimental data.

All the values of axial dispersion coefficients obtained are presented in Table 3. The calculated values of Péclet numbers (Table 4) indicate that gas flow is neither ideal plug flow nor perfect mixing in tested system.

Table 3  
Values of axial dispersion coefficients

| P, Pa             | $V_{imp}, m^3; t_p, s$     |                      |                      |                            |                      |                      | Number of zone; <i>i</i> -th zone | $F_v, m^3/s$         |
|-------------------|----------------------------|----------------------|----------------------|----------------------------|----------------------|----------------------|-----------------------------------|----------------------|
|                   | $2.50 \cdot 10^{-7}; 0.75$ |                      |                      | $5.00 \cdot 10^{-7}; 1.50$ |                      |                      |                                   |                      |
|                   | T, K                       |                      |                      |                            |                      |                      |                                   |                      |
|                   | 313                        | 333                  | 353                  | 313                        | 333                  | 353                  |                                   |                      |
| $D_{L,i}, m^2/s$  |                            |                      |                      |                            |                      |                      |                                   |                      |
| $1.20 \cdot 10^5$ | $7.99 \cdot 10^{-5}$       | $8.45 \cdot 10^{-5}$ | $9.29 \cdot 10^{-5}$ | $7.73 \cdot 10^{-5}$       | $8.51 \cdot 10^{-5}$ | $9.38 \cdot 10^{-5}$ | 1                                 | $3.33 \cdot 10^{-7}$ |
|                   | $2.75 \cdot 10^{-3}$       | $3.53 \cdot 10^{-3}$ | $3.63 \cdot 10^{-3}$ | $2.47 \cdot 10^{-3}$       | $2.71 \cdot 10^{-3}$ | $2.80 \cdot 10^{-3}$ | 2; 3                              |                      |
| $2.00 \cdot 10^5$ | $4.95 \cdot 10^{-5}$       | $5.27 \cdot 10^{-5}$ | $5.71 \cdot 10^{-5}$ | $4.91 \cdot 10^{-5}$       | $5.30 \cdot 10^{-5}$ | $5.65 \cdot 10^{-5}$ | 1                                 |                      |
|                   | $1.44 \cdot 10^{-3}$       | $1.40 \cdot 10^{-3}$ | $1.38 \cdot 10^{-3}$ | $9.42 \cdot 10^{-4}$       | $8.46 \cdot 10^{-4}$ | $7.27 \cdot 10^{-4}$ | 2; 3                              |                      |
| $3.00 \cdot 10^5$ | $3.35 \cdot 10^{-5}$       | $3.50 \cdot 10^{-5}$ | $3.77 \cdot 10^{-5}$ | $3.43 \cdot 10^{-5}$       | $3.61 \cdot 10^{-5}$ | $3.74 \cdot 10^{-5}$ | 1                                 |                      |
|                   | $1.04 \cdot 10^{-3}$       | $1.26 \cdot 10^{-3}$ | $1.26 \cdot 10^{-3}$ | $6.91 \cdot 10^{-4}$       | $7.34 \cdot 10^{-4}$ | $7.80 \cdot 10^{-4}$ | 2; 3                              |                      |

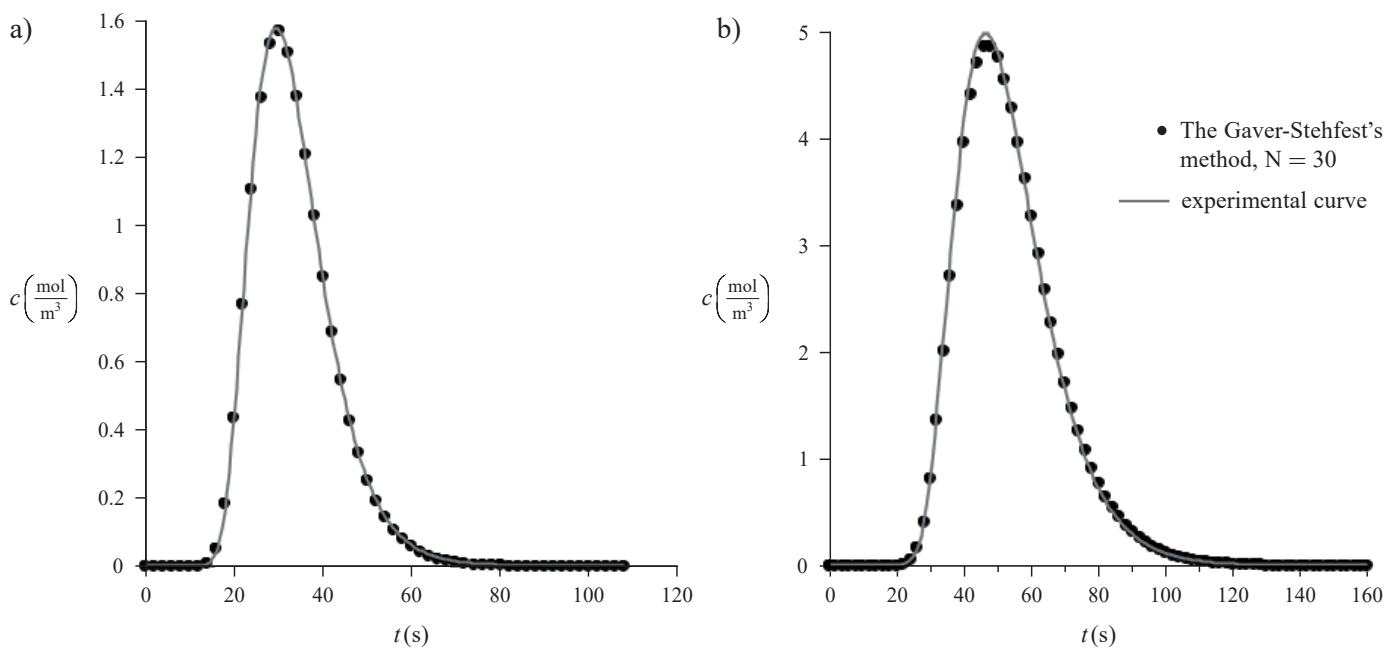


Fig. 2. Numerical and experimental profiles of gas concentration: a)  $P = 1.20 \cdot 10^5$  Pa,  $T = 333$  K,  $V_{imp} = 2.50 \cdot 10^{-7} m^3$ ,  $F_v = 3.33 \cdot 10^{-7} m^3/s$ ,  $t_p = 0.75$  s; b)  $P = 2.00 \cdot 10^5$  Pa,  $T = 353$  K,  $V_{imp} = 5.00 \cdot 10^{-7} m^3$ ,  $F_v = 3.33 \cdot 10^{-7} m^3/s$ ,  $t_p = 1.50$  s

Table 4  
Values of Péclet numbers

| P, Pa                  | V <sub>imp</sub> , m <sup>3</sup> ; t <sub>p</sub> , s |     |     |                                |     |     | Number of zone;<br>i-th zone | F <sub>v</sub> , m <sup>3</sup> /s |
|------------------------|--|-----|-----|--------------------------------|-----|-----|------------------------------|------------------------------------|
|                        | 2.50 · 10 <sup>-7</sup> ; 0.75                         |     |     | 5.00 · 10 <sup>-7</sup> ; 1.50 |     |     |                              |                                    |
|                        | T, K   |     |     |                                |     |     |                              |                                    |
|                        | 313  | 333 | 353 | 313                            | 333 | 353 |                              |                                    |
| Pe <sub>i</sub>        |  |     |     |                                |     |     |                              |                                    |
| 1.20 · 10 <sup>5</sup> | 18   | 18  | 17  | 18                             | 18  | 17  | 1                            | 3.33 · 10 <sup>-7</sup>            |
|                        | 14   | 11  | 12  | 15                             | 15  | 15  | 2                            |                                    |
|                        | 42   | 35  | 36  | 47                             | 46  | 47  | 3                            |                                    |
| 2.00 · 10 <sup>5</sup> | 17   | 17  | 17  | 17                             | 17  | 17  | 1                            |                                    |
|                        | 16   | 17  | 19  | 24                             | 29  | 35  | 2                            |                                    |
|                        | 48   | 53  | 36  | 74                             | 88  | 108 | 3                            |                                    |
| 3.00 · 10 <sup>5</sup> | 17   | 17  | 17  | 17                             | 17  | 17  | 1                            |                                    |
|                        | 15   | 13  | 14  | 22                             | 22  | 22  | 2                            |                                    |
|                        | 45   | 39  | 42  | 67                             | 67  | 67  | 3                            |                                    |

The value of axial dispersion coefficient rises with temperature approximately proportional to the three-halves power of temperature i.e. products of the coefficient and the minus three-halves power of temperature should be equal. The value of axial dispersion coefficient decreases approximately linearly with pressure increase i.e. products of the coefficient and pressure should be equal. The results are presented in Table 5 and 6. Relative differences between calculated values of the products and their mean values for the same operating conditions (with the exception of pressure or temperature, respectively) are smaller than 6.5%, the results agree very well with the theory.

## 5. Conclusions

The method for determining parameters of gas flow motion (e.g. axial dispersion coefficient and Péclet number) is fast and precise. The proposed technique shows remarkable versatility. It can be applied for different temperatures and pressures. The latter is a special advantage of the method under question.

Table 5  
Values of products of  $D_L$  and pressure

| P, Pa  | V <sub>imp</sub> , m <sup>3</sup> ; t <sub>p</sub> , s |       |       |                                |       |       | Number of zone;<br>i-th zone | F <sub>v</sub> , m <sup>3</sup> /s |
|--|--|-------|-------|--------------------------------|-------|-------|------------------------------|------------------------------------|
|  | 2.50 · 10 <sup>-7</sup> ; 0.75                         |       |       | 5.00 · 10 <sup>-7</sup> ; 1.50 |       |       |                              |                                    |
|  | T, K   |       |       |                                |       |       |                              |                                    |
|  | 313  | 333   | 353   | 313                            | 333   | 353   |                              |                                    |
| D <sub>L,i</sub> · P, (m <sup>2</sup> /s · Pa) |  |       |       |                                |       |       |                              |                                    |
| 1.20 · 10 <sup>5</sup>                         | 9.6  | 10.1  | 11.1  | 9.3                            | 10.2  | 11.3  | 1                            | 3.33 · 10 <sup>-7</sup>            |
|  | 330.0  | 423.6 | 435.6 | 296.4                          | 325.2 | 336.0 | 2; 3                         |                                    |
| 2.00 · 10 <sup>5</sup>                         | 9.9  | 10.5  | 11.4  | 9.8                            | 10.6  | 11.3  | 1                            |                                    |
|  | 288.0  | 280.0 | 276.0 | 188.4                          | 169.2 | 145.4 | 2; 3                         |                                    |
| 3.00 · 10 <sup>5</sup>                         | 10.1   | 10.5  | 11.3  | 10.3                           | 10.8  | 11.2  | 1                            |                                    |
|  | 312.0  | 378.0 | 378.0 | 207.3                          | 220.2 | 234.0 | 2; 3                         |                                    |

Table 6  
Values of products of  $D_L$  and the minus three-halves power of temperature

| P, Pa   | V <sub>imp</sub> , m <sup>3</sup> ; t <sub>p</sub> , s |                         |                         |                                |                         |                         | Number of zone;<br>i-th zone | F <sub>v</sub> , m <sup>3</sup> /s |
|---|--|-------------------------|-------------------------|--------------------------------|-------------------------|-------------------------|------------------------------|------------------------------------|
|   | 2.50 · 10 <sup>-7</sup> ; 0.75                         |                         |                         | 5.00 · 10 <sup>-7</sup> ; 1.50 |                         |                         |                              |                                    |
|   | T, K   |                         |                         |                                |                         |                         |                              |                                    |
|   | 313  | 333                     | 353                     | 313                            | 333                     | 353                     |                              |                                    |
| D <sub>L,i</sub> · (1/T) <sup>3/2</sup> , (m <sup>2</sup> /s · K <sup>3/2</sup> ) |  |                         |                         |                                |                         |                         |                              |                                    |
| 1.20 · 10 <sup>5</sup>  | 1.44 · 10 <sup>-8</sup>                                | 1.39 · 10 <sup>-8</sup> | 1.40 · 10 <sup>-8</sup> | 1.40 · 10 <sup>-8</sup>        | 1.40 · 10 <sup>-8</sup> | 1.41 · 10 <sup>-8</sup> | 1                            | 3.33 · 10 <sup>-7</sup>            |
|   | 4.97 · 10 <sup>-7</sup>                                | 5.81 · 10 <sup>-7</sup> | 5.47 · 10 <sup>-7</sup> | 4.46 · 10 <sup>-7</sup>        | 4.46 · 10 <sup>-7</sup> | 4.22 · 10 <sup>-7</sup> | 2; 3                         |                                    |
| 2.00 · 10 <sup>5</sup>  | 8.94 · 10 <sup>-9</sup>                                | 8.67 · 10 <sup>-9</sup> | 8.61 · 10 <sup>-9</sup> | 8.87 · 10 <sup>-9</sup>        | 8.72 · 10 <sup>-9</sup> | 8.52 · 10 <sup>-9</sup> | 1                            |                                    |
|   | 2.60 · 10 <sup>-7</sup>                                | 2.30 · 10 <sup>-7</sup> | 2.08 · 10 <sup>-7</sup> | 1.39 · 10 <sup>-7</sup>        | 1.39 · 10 <sup>-7</sup> | 1.10 · 10 <sup>-7</sup> | 2; 3                         |                                    |
| 3.00 · 10 <sup>5</sup>  | 6.05 · 10 <sup>-9</sup>                                | 5.76 · 10 <sup>-9</sup> | 5.68 · 10 <sup>-9</sup> | 6.19 · 10 <sup>-9</sup>        | 5.94 · 10 <sup>-9</sup> | 5.64 · 10 <sup>-9</sup> | 1                            |                                    |
|   | 1.88 · 10 <sup>-7</sup>                                | 2.07 · 10 <sup>-7</sup> | 1.90 · 10 <sup>-7</sup> | 1.25 · 10 <sup>-7</sup>        | 1.21 · 10 <sup>-7</sup> | 1.18 · 10 <sup>-7</sup> | 2; 3                         |                                    |

The method requires complex mathematical manipulations (mathematical formulas of Laplace-domain model are rather sophisticated) and the symbolic computing environment avoids mistakes. Hence, the CAS-type program were employed. The required numerical calculations were conducted using the same program.

It should be pointed out that the method can be easily adapted to other gas flow system: (i) the scheme of finding complex function that describe outlet concentration is the same; (ii) the numerical algorithm can be the same. Differences can arise in a number of zones or dimensions of measurement unit parts.

**Acknowledgements.** The authors would like to thank W. Próchniak and P. Wiercioch from New Chemical Synthesis Institute, Pulawy (Poland) for sharing the experimental data.

## REFERENCES

- [1] F. Yang, X. Wang, and H. Liu, "Application of Laplace transform in well test interpretation-an example of the field cavity-fractured reservoirs in tarim basin", 2011 International Conference on Multimedia Technology, IEEE, Hangzhou, China, 1988–1991, 2011.
- [2] C. Montella, "LSV modelling of electrochemical systems through numerical inversion of Laplace transforms, I: The GSLSV algorithm", *J. Electroanal. Chem.*, 614(1–2), 121–130 (2008).
- [3] R.M. Endah and S.D. Surjanto, "Performance of Gaver-Stehfest numerical Laplace inversion method on option pricing formulas", *Int. J. Appl. Math. Comput. Sci.*, 3(2), 71–76 (2017).
- [4] J.H.Knight and A.P. Raiche, "Transient electromagnetic calculations using the Gaver-Stehfest inverse Laplace transform method", *Geophysics*, 47(1), 47–50 (1982).
- [5] N.Smith and L. Brančik, "Comparative study on one-dimensional numerical inverse Laplace transform methods for electrical engineering", *Elektrorevue*, 18(1), 1–6 (2016).
- [6] I. Kocabas, "Application of iterated Laplace transformation to tracer transients in heterogeneous porous media", *J. Franklin. Inst.*, 348(7), 1339–1362 (2011).
- [7] Q. Wang and H. Zhan, "On different numerical inverse Laplace methods for solute transport problems", *Adv Water Resour*, 75, 80–92 (2015).
- [8] L.-W. Chiang, "The application of numerical Laplace inversion methods to groundwater flow and solute transport problems", New Mexico Institute of Mining and Technology, Socorro, New Mexico, 1989.
- [9] F.H. Escobar, F.A. Leguizamo, and J.H. Cantillo, "Comparison of Stehfest's and Iseger's algorithms for Laplacian inversion in pressure well tests", *J. Eng. Appl. Sci.*, 9(6), 919–922 (2014).
- [10] J.S. Chen, C.W. Liu, C.S. Chenb, and H.D. Yehc, "A Laplace transform solution for tracer tests in a radially convergent flow field with upstream dispersion", *J. Hydrol.*, 183(3–4), 263–275 (1996).
- [11] K. Boupfa, J.M. Jacobs, and K. Hartfield, "MDL Groundwater software: Laplace transforms and the De Hoog algorithm to solve contaminant transport equation", *Computers & Geosciences*, 30(5), 445–453 (2004).
- [12] O. Taiwo, J. Schultz, and V. Krebs, "A comparison of two methods for the numerical inversion of Laplace transforms", *Computers Chem. Eng.*, 19(3), 303–308 (1995).
- [13] O. Taiwo and R. King, "Determination of kinetic parameters for the adsorption of a protein on porous beads using symbolic computation and numerical Laplace inversion", *Chem Eng. Proc.*, 42(7), 561–568 (2003).
- [14] P. Wyns, D.P. Foty, and K.E. Oughstun, "Numerical analysis of the precursor fields in linear dispersive pulse propagation", *J. Opt. Soc. Am.*, 6(9), 1421–1429 (1989).
- [15] M. Wójcik, M. Szukiewicz, P. Kowalik, and W. Próchniak, "The efficiency of the Gaver-Stehfest method to solve one-dimensional gas flow model", *Adv. Sci. Technol. Res. J.*, 11(1), 246–252 (2017).
- [16] M. Wójcik, M. Szukiewicz, and P. Kowalik, "Application of numerical Laplace inversion methods in chemical engineering with Maple<sup>®</sup>", *J. Appl. Comput. Sci. Meth.*, 7(1), 5–15 (2015).